

The Impact of Bandwidth on Through-the-wall Radar Imaging

Huamei ZHANG

School of Electronic Science and Engineering, Nanjing University of Posts and Telecommunications,
Nanjing 210003, China
Tel.: 86-25-85866409
E-mail: zhanghm@njupt.edu.cn

Received: 26 April 2014 /Accepted: 29 April 2014 /Published: 30 April 2014

Abstract: An electromagnetic model is simulated using finite difference time domain for through-the-wall radar imaging. In the numerical simulation narrow-, wide-, and ultra-wide-band signals are used as emission sources. The back projection algorithm is applied to image square and rectangular ideal metal bodies based on a refraction model. The results demonstrate that there is obvious refraction in the through-the-wall propagation of electromagnetic waves. For the calculation of propagation delay, the variation in propagation path and time must be taken into account. Then the actual refractive point is found accurately and rapidly according to Fermat's principle. For imaging, all three signal sources can be used to acquire the image. The image result is best for the ultra-wide band and worst for the narrow-wide band. For the azimuth, synthetic aperture technique is adopted to achieve high resolution. For the range, there is a positive proportional relationship between the resolution and signal bandwidth. The wide band signal significantly increases the range resolution. Therefore, ultra-wide band SAR radar has more precise imaging and positioning capabilities. Copyright © 2014 IFSA Publishing, S. L.

Keywords: Through-the-wall imaging, Ultra-wide band, Back projection algorithm, Finite difference time domain, Refraction model.

1. Introduction

Through-the-wall imaging is a novel non-destructive detection technology that can quickly and accurately locate objects behind obstacles and analyze their states. It plays a very important role in military operations, antiterrorism, firefighting, and rescue missions after earthquakes, drawing ever more attention from the scientific community, local and foreign governments, and the public [1-3].

Most previous radar imaging techniques have used large-distance space-borne radar or aircraft-borne radar with distances between the radar and targets of over 1000 km, or at least several km. In these cases, the target is located in the far field range of the radar antenna, which satisfies the far field condition. In addition, the spherical wave can be

approximated as a plane wave, and there is a relatively clear correspondence between the phase of the target echo and the location of the target. For near-field-like through-the-wall imaging, the distance between the radar and the target is only several to tens of meters. The target is located in the near field of the antenna; thus, the spherical wave cannot be approximated as a planar wave. The distribution of the electromagnetic field is also very complicated. As a result, the near-field problem cannot be resolved by the methods used for far field. Therefore, we must find a new approach to analyze near-field radar.

For near-field radar imaging, most studies have imaged ideal point targets using Synthetic Aperture Radar (SAR). This method of analysis is based on signal processing. It implements two-dimensional Fourier transform and an inverse transform for the

signals after matched filtering. However, the velocity of the signal changes during through-the-wall propagation. Thus, it is difficult to determine the propagation path, which makes imaging difficult. Moreover, this model cannot truly reflect the actual model and cannot effectively simulate a non-ideal point target. Therefore, we have adopted the finite difference time domain (FDTD) method to establish a simulation model for the full electromagnetic field and apply the coherent time-domain method, i.e., the back projection (BP) algorithm, for imaging [4-8]. The advantages of the BP algorithm in comparison with other traditional frequency-domain methods are that it does not need to consider the Doppler shift and that it uses a simple time-delay computation to replace the complicated Fourier transform.

The quality of through-the-wall radar imaging is related to the selection of the signal source. Signal sources can be roughly divided into three classes: narrow band (NB) signals, wide band (WB) signals, and ultra-wide band (UWB) signals. According to the definition of percentage bandwidth:

$$BW = 2(f_H - f_L)/(f_H + f_L) \quad (1)$$

The narrow band occurs when $BW < 1\%$, the wide band occurs when $1\% < BW < 25\%$, and the ultra-wide band occurs when $BW > 25\%$. There is a proportional relationship between the range resolution and the bandwidth of the signal. More specifically, the range resolution is higher when the bandwidth of the signal is wider and lower when the bandwidth is narrower. Owing to their relatively high range resolution and relatively good recognition performance, WB and UWB signals are being implemented in an increasing number of applications [9].

In this paper, we use NB, WB, and UWB signals as emission sources and analyze the scattering mechanism of the targets and the refraction phenomenon of the electromagnetic waves used to image and determine the positions of targets.

2. Imaging Algorithm

Most imaging algorithms perform signal processing based on the frequency-domain Fourier transform and inverse transform. For through-the-wall radar, the signal must propagate through different media. As a result, it is difficult to implement the Fourier transform and inverse transform. The BP algorithm [4, 7] is a time-domain algorithm that is not related to the frequency domain. It can eliminate the effect of the Doppler shift through the time delay, which significantly simplifies the calculation. In addition, the accuracy of the BP algorithm is high. Therefore, the BP algorithm is cost-effective for analyzing through-the-wall radar signals.

The BP algorithm is based on computed-tomography technology. It uses the data of the

imaging process from the antenna array. In the process of forward modeling, we derive the temporal variation of the field intensity in the imaging region. By subtracting the field values with the targets from the field values without the targets, we can derive the scattering echo data for the targets. We can then derive an image of the targets through the BP calculation of the scattered echo waves.

The procedure for imaging using the BP algorithm is as follows:

- 1) Divide the entire imaging domain into spatial grids;
- 2) For each grid, calculate the round-trip delay from the transmitter to the grid and from the grid to the receiver;
- 3) Record the electric field value at the location of the receiver;
- 4) For each grid, repeat steps 2 and 3;
- 5) On each grid, sum the magnitude of the electric fields.

In free space, the imaging function is

$$I(x, y) = \sum_n E(t(n)), \quad (2)$$

where

$$t(n) = [R_t(n) + R_r(n)]/c, \quad (3)$$

where $t(n)$ is the round-trip time delay from the transmitter to the target and then from the target to the receiver, $E(t(n))$ is the field value received by the receiver, c is the speed of the electromagnetic wave in free space, $R_t(n)$ is the distance from the receiver to the target, and $R_r(n)$ is the distance from the target to the receiver.

3. Propagation Refraction Model

Due to the presence of a wall, the velocity of electromagnetic waves will change, as will the direction of propagation, resulting in refraction. This phenomenon causes considerable difficulties for precise imaging. Therefore, we must find the exact refractive point and add a compensation value to the time [4, 10]. Precise compensation plays a very important role in the imaging result. Without proper compensation, there will be deviation in the imaging. Some studies have determined the refractive point by solving the quartic equation with one unknown. This principle is easy to understand, but the process is very time-consuming. According to Fermat's principle, the time is shortest for the electromagnetic wave to propagate along the actual path. Therefore, we look for the shortest time to find the refractive point, which is easy to achieve and can substantially simplify the calculation. The detailed procedures are described below.

Let us first consider that there are not multiple reflections between the interfaces and establish the refraction model of electromagnetic wave propagation shown in Fig. 1. The propagation time from the transmission antenna to the target is calculated. Then the location of the transmitting antenna, target, and two refractive points to be (x_b, y_l) , (x, y) , $(x_1, -d_w)$, and $(x_2, 0)$ are set respectively, giving the model shown in Fig. 1.

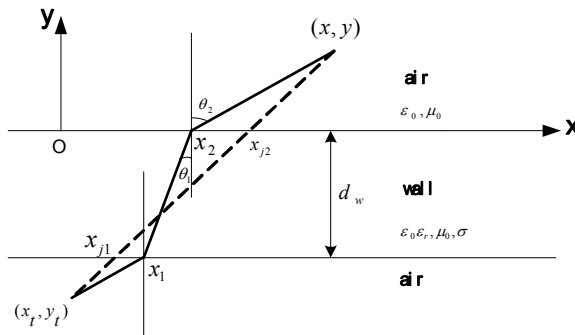


Fig. 1. Through-the-wall propagation model of the electromagnetic waves.

The propagation distance of the signal in the wall is:

$$l_1 = \sqrt{(x_1 - x_2)^2 + d_w^2}, \quad (4)$$

the propagation distance of the signal in air is

$$l_2 = \sqrt{(x - x_2)^2 + y^2}, \quad (5)$$

$$l_3 = \sqrt{(x_t - x_1)^2 + (y_t + d_w)^2}, \quad (6)$$

According to the given electromagnetic parameters, we next determine whether $\sigma/\omega\epsilon$ is far below 1. If it is, we can approximate the concrete wall as a good medium, and the propagation speed of the electromagnetic waves in the wall will be approximately $v = c/\sqrt{\epsilon_r}$, where ϵ_r is the relative dielectric constant of the wall. The total propagation time of the signal from the transmission antenna to the target is given by the following expression,

$$t_t(n) = (\sqrt{\epsilon_r} l_1 + l_2 + l_3) / c, \quad (7)$$

For real-time imaging, we must rapidly identify the refraction point. However, the process of looking for the refraction point takes a long time. Based on our analysis, the relative dielectric constant of the wall is always greater than 1. According to the refraction theorem, $\theta_2 > \theta_1$. When we connect points (x_t, y_t) and (x, y) , the line will intersect with the upper and lower wall surfaces at two points, i.e., $(x_{j2}, 0)$,

and $(x_{j1}, -d_w)$. Thus, x_1 and x_2 must be between x_{j1} and x_{j2} . This positioning shortens the time, allowing rapid and accurate determination of the refraction point, thereby improving the imaging efficiency.

With the same method, we can derive the propagation time from the target to the receiving antenna, t_{xyr} . Accordingly, we can calculate the time delay of the echo signal from the transmitting antenna to every receiving antenna, $t_{xyt} + t_{xyr}$.

The imaging function at this time is as follows,

$$I(x, y) = \sum_n E(t_{xyt} + t_{xyr}), \quad (8)$$

4. Simulation Model

4.1. Room Model

The simulation model for a single wall is shown in Fig. 2. The room is 3.2 m long and 3 m wide. To simplify the model, we presume that the wall is a uniform non-dispersive medium made of 0.1 m-thick concrete. At 1 GHz, the relative dielectric constant (ϵ_r) of the wall is 6, and the conductivity (σ) is 0.00195. When $\sigma/\omega\epsilon = 0.0058 \ll 1$, we can use the conclusion of section 3 for analysis. The excitation source is placed at the center of the long side at a distance of 0.05 m from the wall.

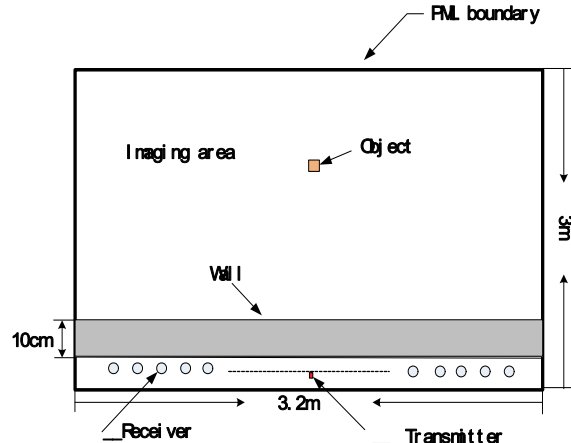


Fig. 2. FDTD simulation model.

We use the two-dimensional FDTD method for the simulation. The size of the grid is 0.01 m, and the time interval is 16.7 ps.

4.2. NB Signal, WB Signal, and UWB Signal

The NB signal is a modulated sine wave. The central frequency is 1 GHz, the 3 dB bandwidth is 2 MHz and the percentage of the bandwidth is 0.2 %, making it a NB signal.

The WB signal is a modulated Gaussian pulse wave. The central frequency is 1 GHz, the pulse width is 9 ns, The 3 dB bandwidth is 180 MHz and the percentage of the bandwidth is 18 %, making it a WB signal.

The UWB signal is a modulated Gaussian pulse wave. The central frequency is 1 GHz, the pulse width is 1.2 ns, The 3 dB bandwidth is 1.25 GHz and the percentage of the bandwidth is 125 %, which makes it an UWB signal.

5. BP Imaging and Discussion

To achieve high resolution in the azimuth, we adopt the SAR technique. On two sides of the signal source, we symmetrically arrange 120 receivers, which are separated by 0.02 m. We use square and rectangular metal bodies as the targets for imaging. The square metal body is 0.11 m wide. Its central location is at (1.9 m, 1.9 m). The rectangular metal body is 0.8 m long and 0.1 m wide. Its central location is at (2 m, 1.9 m). Because imaging of the square body is similar as imaging of the rectangular body, only the results of the latter is given below in order to save the length.

5.1. Imaging Results for the NB Source

When the NB signal is used as a signal source, the result is shown in Fig. 3.

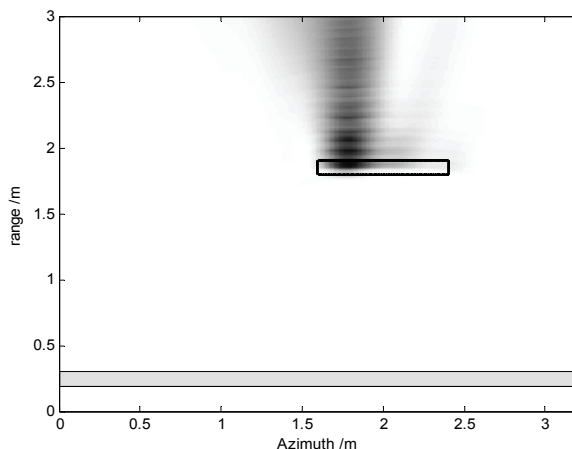


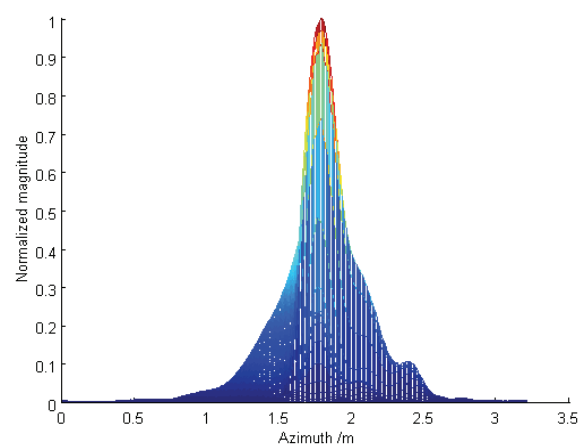
Fig. 3. The BP near-field image results for the NB signal source.

As shown in Fig. 3, the imaging only sees the tip location of the targets. In addition, the defocusing phenomenon is very serious behind the target.

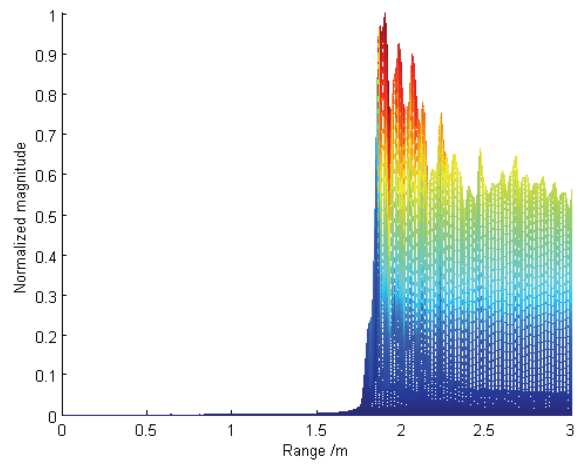
Fig. 4 shows the distribution of the normalized magnitude for the azimuth and range.

From Fig. 4(a), the position of the target and the length of azimuth are generally consistent with the actual target, because in the azimuth, we adopt multiple receivers to form the SAR. Therefore, the

resolution in the azimuth is relatively high. There is only a defocusing phenomenon and diffusion of part of the signal energy. Fig. 4(b) shows that the resolution in the range direction is very low because of the NB signal. The defocusing phenomenon is significant, and further signal energy is lost. Therefore, during through-the-wall imaging, we must enhance the emission energy. However, through-the-wall imaging is a near-field detection technique, and the target to be detected could also be human. Therefore, it is desirable to employ smaller transmission energies. Based on these criteria, the NB technique is not suitable for near-distance detection and imaging of targets.



(a) Azimuth of the rectangular metal body.



(b) Range of the rectangular metal body.

Fig. 4. Distribution of the magnitude with the NB signal source.

5.2. Imaging Results for the WB Source

Fig. 5 shows the results using the WB signal as the signal source.

As shown in Fig. 5, there are multiple ripples in the imaging position, which are caused by the multiple peak points of the WB signal. It is thus

difficult to use this mode for the precise positioning of targets.

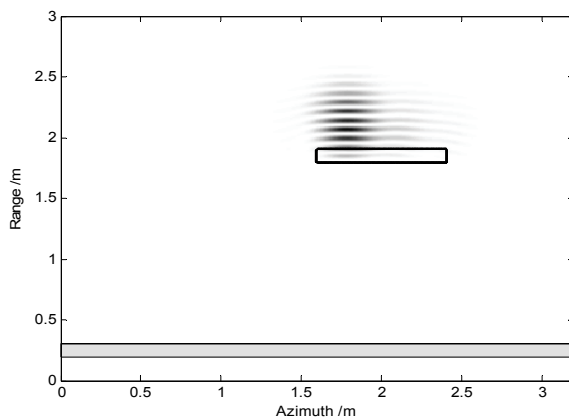
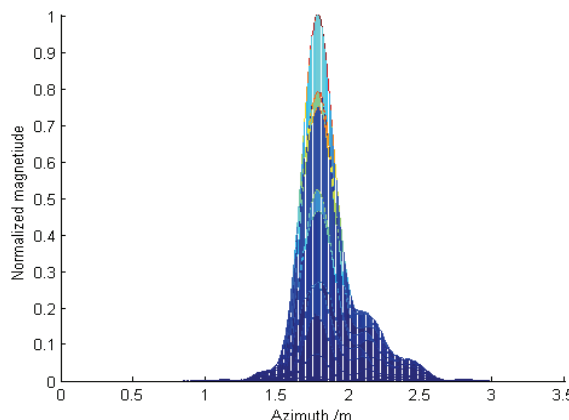
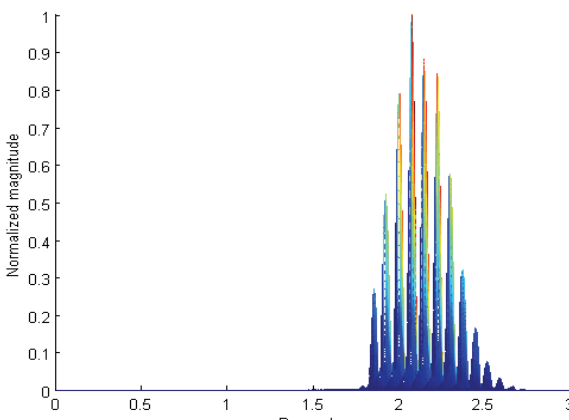


Fig. 5. The BP near-field image results for the WB signal source.

Fig. 6 shows the distribution of the normalized magnitude in the azimuth and range direction.



(a) Azimuth of the rectangular metal body.



(b) Range of the rectangular metal body.

Fig. 6. Distribution of the magnitude with the WB signal source.

We can see the level of resolution from the beam width. In Figs. 6(a), not only can we determine the position of the targets in the azimuth, but we can also determine their length. From Fig. 6(b), we know that because of the WB signal, the multiple peaks significantly reduce the range resolution. Thus, this method generally cannot determine the position and shape of the targets in the range.

5.3. Imaging Results for the UWB Source

For the UWB signal, the results are shown in Fig. 7.

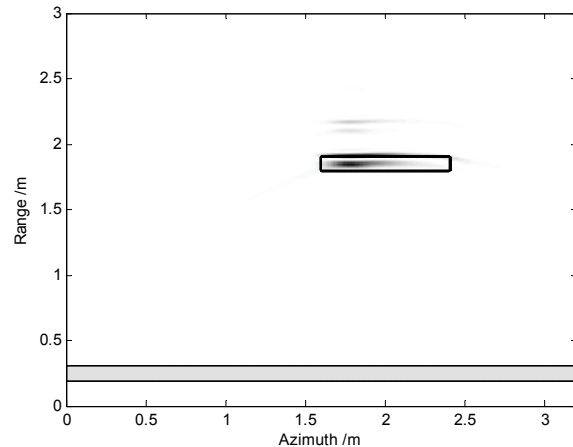


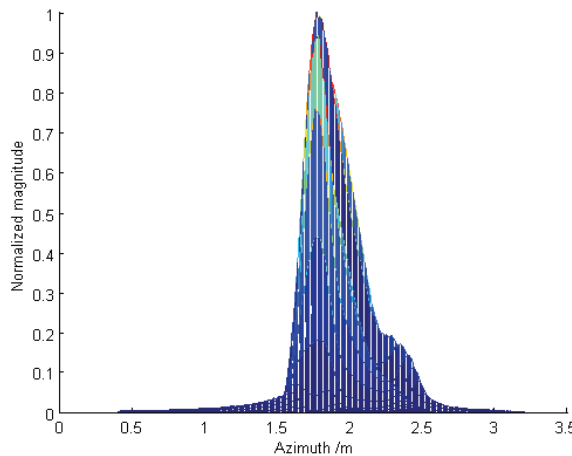
Fig. 7. The BP near-field image results for the UWB signal source.

According to Fig. 7, the imaging position is in good agreement with the actual position of metal body. The imaging shape is also essentially consistent with the target.

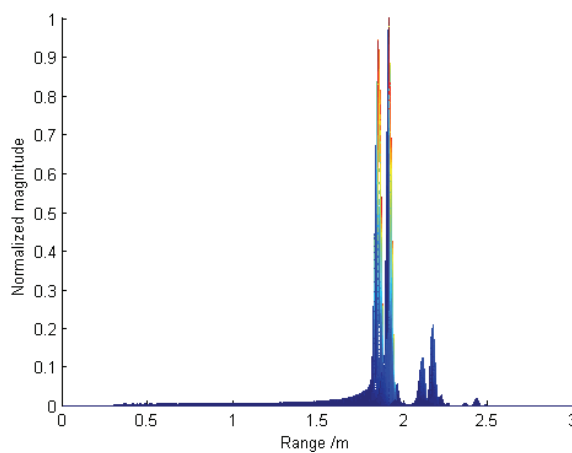
Fig. 8 shows the distribution of the normalized magnitude for the azimuth and range.

According to the magnitude distribution in Fig. 8, for the range and azimuth of the rectangular metal body, the imaging position is in good agreement with the position of the target. The size of the image is also consistent with the actual size of the target. Moreover, the energy of the signal is almost completely concentrated at the target. There is essentially no defocusing phenomenon in the azimuth. The defocusing phenomenon is also not significant for the range and does not affect the positioning of the targets.

In comparison with the NB through-the-wall radar, the WB radar can significantly reduce the transmission power. In comparison with WB radar, the UWB radar can achieve high-resolution imaging not only for the azimuth but also for the range. Therefore, the UWB radar efficiently images and determines the positioning of targets.



(a) Azimuth of the rectangular metal body.



(b) Range of the rectangular metal body.

Fig. 8. Distribution of the magnitude for with the UWB signal source.

To more intuitively reflect the impact of the signal bandwidth on through-the-wall imaging, we give the percentage of signal energy of the square metal body and the rectangular metal body at the location of the target in the range relative to the total energy in Table 1.

Table 1. Percentage of the signal energy at the target location in the range relative to the total energy.

	NB signal	WB signal	UWB signal
Square body	9.3 %	9.0 %	50.4 %
Rectangular body	7.8 %	6.1 %	46.2 %

From Table 1, we can clearly see that if the bandwidth of the signal is wider, the percentage of the signal energy at the target location relative to the total energy is higher. This phenomenon indicates that if the bandwidth is wider, the signal energy is more concentrated at the target, which provides the

possibility for low-power transmission, thus reducing the electromagnetic radiation toward the target to allow non-destructive detection.

Meanwhile, we also give the percentage of the signal energy of signal energy of the square metal body and the rectangular metal body at the target location in the azimuth relative to the total energy, as shown in Table 2.

Table 2. Percentage of signal energy at the target location in the azimuth relative to the total energy.

	NB signal	WB signal	UWB signal
Square body	23.2 %	33.0 %	34.6 %
Rectangular body	83.7 %	90.1 %	87.8 %

As shown in Table 2, the percentage of signal energy at the target position in the azimuth direction relative to the total energy is not only related to the signal bandwidth but also depends considerably on the size of the targets. When there is a WB or UWB signal, there is no significant difference in the energy concentration and it is much higher than the degree of energy concentration for NB. Whatever the signal is, the energy concentration for large targets is much higher than for small targets, which indicates that the large targets are more easily detected.

Moreover, although the bandwidth of the three signals is different, the algorithm is consistent, and thus the cost of the calculation is the same.

By comparing Figs. 4, 6, and 8, we can see that in comparison with the NB, WB and UWB signals, the range resolution using the UWB signal is significantly greater. That is, the range resolution is higher if the bandwidth of the signal is wider. The UWB signal has higher range resolution due to its wider bandwidth. The resolution of the azimuth is related to the length of the synthetic aperture. If the length of the aperture is longer, the resolution of the azimuth is higher. In this paper, we adopt a technique for deploying multiple receivers to simulate the SAR, which can achieve the requirement for a high resolution of the azimuth.

Therefore, the UWB signal has the advantage of a wider bandwidth. By combining the UWB signal with the SAR technique, we can achieve very high 2D resolution, which enables precise positioning and imaging. As a result, UWB imaging radar has been applied to an increasing number of applications in both the military and civilian domains.

6. Conclusions

For through-the-wall radar imaging, we applied the FDTD method to simulate the full-electromagnetic field in the near-field model. We used NB, WB, and UWB signals as the transmission

sources and analyzed the imaging results for square metal bodies and rectangular metal bodies. By comparing the imaging results, we found that, with the inclusion of a wall, the UWB, NB, and WB sources can achieve satisfactory imaging results. The results for the UWB source were best, followed by the WB source and the NB source. In the azimuth, we can achieve very high resolution using the SAR technique. Due to the different signal bandwidths, the resolution range is varied. Due to its very broad bandwidth, the UWB signal had a higher resolution for the range than the NB and WB signals. Thus, the UWB signal can efficiently determine the position and shape of targets. In conclusion, UWB SAR radar is more suitable for precise near-distance positioning and imaging than other techniques.

References

- [1]. Bolomey J. C., Recent European developments in active microwave imaging for industrial, scientific, and medical applications, *IEEE Transactions on Microwave Theory and Techniques*, Vol. 35, Issue 12, pp. 2109-2117.
- [2]. Baranoskie E. J., Through wall imaging: historical perspective and future directions, in *Proceedings of the IEEE International Conference on Acoustics, Speech, and Signal Processing (ICASSP' 08)*, Las Vegas, USA, 30 March – 4 April, 2008, pp. 5173-5176.
- [3]. Mahfouz M., Fathy A., Yang Yunqiang, et al., See-through-wall imaging using ultra wideband pulse systems, in *Proceedings of the 34th Workshop on Applied Imagery and Pattern Recognition (AIPR'05)*, Washington DC, U. S. A., 19-21 October 2005.
- [4]. Gu Xiang, Zhang Yunhua, Autofocus imaging simulation for through-wall radar by using FDTD with unknown wall characteristics, in *Proceedings of the Asia-Pacific Microwave Conference (APMC)*, Yokohama, Japan, 7-10 December 2010, pp. 1657-1660.
- [5]. Jia Yong, Kong Lingjiang, Yang Xiaobo, Improved cross-correlated back-projection algorithm for through-wall-radar imaging, *Radar Conference*, Shanxi, China, 14-16 April 2013, pp. 1-3.
- [6]. Nag S., Barnes M. A., Payment T., et al., An ultra-wideband through-wall radar for detecting the motion of people in real time, in *Proceedings of the International Society for Optics and Photonics*, 2002, Vol. 4744, pp. 48-57.
- [7]. Sylvain G., Eric H., Walid C., Surveillance through concrete walls, *Technical Memorandum DRDC Ottawa TM 2003-233*, Ottawa, Canada, December 2003.
- [8]. Chen Lei, Shan Ouyang, Modified cross-correlated back projection for UWB through-wall surveillance, *International Conference on Wireless Communications, Networking and Mobile Computing*, Shanghai, China, 21-23 September 2007, pp. 516-519.
- [9]. Bao Zheng, Xing Mengdao, Wang Tong, The Technology of Radar Imaging, *Publishing House of Electronics Industry*, 2005. (in Chinese).
- [10]. Chen Lei, Shan Ouyang, Through-wall surveillance using ultra-wideband short pulse radar: numerical simulation, in *Proceedings of the IEEE Conference on Industrial Electronics and Applications*, Harbin, China, 23-25 May 2007, pp. 1551-1554.

2014 Copyright ©, International Frequency Sensor Association (IFSA) Publishing, S. L. All rights reserved.
(<http://www.sensorsportal.com>)

Call for Books Proposals Sensors, MEMS, Measuring instrumentation, etc.

International Frequency Sensor Association Publishing



Benefits and rewards of being an IFSA author:

1) Royalties.

Today IFSA offers most high royalty in the world: you will receive 50 % of each book sold in comparison with 8-11 % from other publishers, and get payment on monthly basis compared with other publishers' yearly basis.

2) Quick Publication.

IFSA recognizes the value to our customers of timely information, so we produce your book quickly: 2 months publishing schedule compared with other publishers' 5-18-month schedule.

3) The Best Targeted Marketing and Promotion.

As a leading online publisher in sensors related fields, IFSA and its Sensors Web Portal has a great expertise and experience to market and promote your book worldwide. An extensive marketing plan will be developed for each new book, including intensive promotions in IFSA's media: journal, magazine, newsletter and online bookstore at Sensors Web Portal.

4) Published Format: pdf (Acrobat).

When you publish with IFSA your book will never go out of print and can be delivered to customers in a few minutes.



You are invited kindly to share in the benefits of being an IFSA author and to submit your book proposal or/and a sample chapter for review by e-mail to editor@sensorsportal.com. These proposals may include technical references, application engineering handbooks, monographs, guides and textbooks. Also edited survey books, state-of-the art or state-of-the-technology, are of interest to us.



The Fifth International Conference on Sensor Device Technologies and Applications



SENSORDEVICES 2014

16 - 20 November 2014 - Lisbon, Portugal

Tracks: Sensor devices - Ultrasonic and Piezosensors - Photonics - Infrared - Gas Sensors - Geosensors - Sensor device technologies - Sensors signal conditioning and interfacing circuits - Medical devices and sensors applications - Sensors domain-oriented devices, technologies, and applications - Sensor-based localization and tracking technologies - Sensors and Transducers for Non-Destructive Testing

Deadline for papers: 20 June 2014

<http://www.iaria.org/conferences2014/SENSORDEVICES14.html>



The Eighth International Conference on Sensor Technologies and Applications



**Deadline for papers:
20 June 2014**

SENSORCOMM 2014

16 - 20 November 2014 - Lisbon, Portugal

Tracks: Architectures, protocols and algorithms of sensor networks - Energy management and control of sensor networks - Resource allocation, services, QoS and fault tolerance in sensor networks - Performance, simulation and modelling of sensor networks - Security and monitoring of sensor networks - Sensor circuits and sensor devices - Radio issues in wireless sensor networks - Software, applications and programming of sensor networks - Data allocation and information in sensor networks - Deployments and implementations of sensor networks - Under water sensors and systems - Energy optimization in wireless sensor networks

<http://www.iaria.org/conferences2014/SENSORCOMM14.html>



The Seventh International Conference on Advances in Circuits, Electronics and Micro-electronics

CENICS 2014

16 - 20 November 2014 - Lisbon, Portugal

Deadline for papers: 20 June 2014

Tracks: Semiconductors and applications - Design, models and languages - Signal processing circuits - Arithmetic computational circuits - Microelectronics - Electronics technologies - Special circuits - Consumer electronics - Application-oriented electronics

<http://www.iaria.org/conferences2014/CENICS14.html>

